Supporting Information

An ultrathin iron-porphyrin based nanocapsule with high

peroxidase-like activity for highly sensitive glucose detection

Xiaotong Fan,[a,b,d,e] Tingting Wang,[a] Shengda Liu,[a] Ruizhen Tian,[a] Liang Wang,[a,b,d] Jiayun Xu,[a] Junqiu Liu,*[a] Min Ma[e] and Zhengzhi Wu*[b,c,d]

a. *State Key Laboratory of Supramolecular Structure and Materials, College of Chemistry, Jilin University, 2699 Qianjin Road, Changchun 130012, China.*

b. *The Fist Affiliated Hospital of Shenzhen University, Shenzhen 518035, China.*

c. *The Eighth Affiliated Hospital of Sun Yat-sen University, Shenzhen 518033, China*

d. *Shenzhen Institute of Geriatrics, Shenzhen 518020, China.*

e. *Integrated Chinese and Western Medicine Postdoctoral research station, Jinan University, Guangzhou 510632, China.*

1. Chemicals

Pyrrole, 4-pyridinecarboxaldehyde, iodomethane, 1, 6-dibromhexan, 3, 3, 5, 5-tetramethylbenzidine (TMB) were purchased from Energy Chemical plant and used directly. Glucose oxidase (GOX) was purchased from Sigma-Aldrich. Ferrous chloride tetrahydrate (FeCl$_2$•4H$_2$O), propanoic acid, methanol, ethanol, N, N-dimethylformamide (DMF), arabinose, sucrose, lactose, hydrogen peroxide and glucose were purchased from Beijing Chemical Plant.

2. Instruments

^{1}H NMR spectrum was obtained by Bruker 510 apparatus (500 MHz) using CDCl$_3$ as solvent with tetramethylsilane (TMS) as a reference. Transmission Electron Microscopy (TEM) images were captured with a JEM-2100F instrument at a 200 kV accelerating voltage. Scanning Electron Microscopy (SEM) images were obtained with a JEOL JSM 6700F apparatus. Mass spectrometry was operated using liquid chromatograph-mass spectrometer (LC-MS, Agilent1290-micrOTOF-Q Ⅱ) with the solvent of methanol. UV-Vis spectra were recorded using Shimadzu 3100 UV-VIS-NIR Recording Spectrophotometer. Ultrafiltration tubes were purchased from sartorius.

3. Synthesis of the monomers
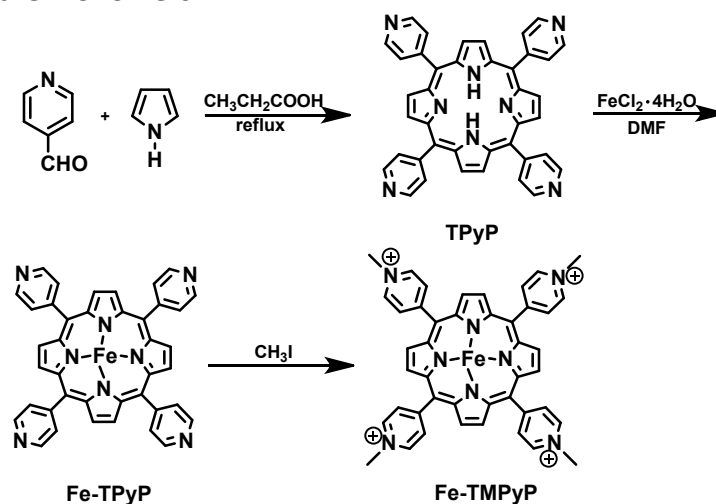
Scheme S1 The synthetic route of TPyP, Fe-TPyP and Fe-TMPyP.

Synthesis of 5, 10, 15, 20-tetrakis (4'-pyridyl) porphyrin (TPyP): 4-Pyridinecarboxaldehyde (7.32 g, 60 mmol) and 300 mL of propanoic acid was mixed together, then the mixture was heated to reflux under the condition of nitrogen atmosphere, followed by dropwise adding 50 mL of propanoic acid dissolved pyrrole (4.02 g, 60 mmol). The mixture was refluxed for another 2.5 hours under the condition of nitrogen atmosphere. After cooling to room temperature, about 250 mL of propanoic acid was evaporated by vacuum, and 100 mL of methanol was added into the mixture. The resulting precipitate was filtered and washed several times using ethanol, then dried under vacuum to obtain the purple solid (1.9 g, 3.07 mmol, 20.5%). ^{1}H NMR (CDCl$_3$, 500 MHz): 9.07 (d, 8H), 8.86 (s, 8H), 8.17 (d, 8H), -2.75 (s, 2H). MS (MALDI-MS) = 619.255 [M + H]$^+$.

Synthesis of 5, 10, 15, 20-tetrakis (4'-pyridyl) iron (Ⅲ) porphyrin (Fe-TPyP): The synthetic route was similar to the previous report.[1] Typically, FeCl$_2$•4H$_2$O (600 mg, 3 mmol) was added into the mixture of TPyP (92.7 mg, 0.15 mmol) and DMF (50 mL). Then, the mixture was refluxed for 4 hours under the condition of nitrogen atmosphere. DMF was evaporated by vacuum, and the residue

was purified by column chromatography and dried under vacuum to get the purple product (69.54 mg, 0.095 mmol, 63%). MS (MALDI-MS) = 672.117.

Synthesis of 5, 10, 15, 20-tetrakis (1-methylpyridinium-4'-yl) iron(Ⅲ) porphyrin (Fe-TMPyP): Excess iodomethane was added into the DMF (20 mL) dissolved Fe-TPyP (50 mg, 0.074 mmol) solution. After stirring at room temperature for two days, a large amount of diethyl ether was added and the resulting precipitate was collected (45.75 mg, 0.062 mmol, 83.78%). MS (ESI-MS)=183.06 $[M]^{4+}$.

4. The preparation of nanocapsules

Fe-TPyP (2 mg, 0.0029 mmol) or TPyP (2 mg, 0.0032 mmol) and 1, 6-dibromhexan (20 μL, 0.13 mmol) were dissolved together in 16 mL of DMF. The mixture was refluxed for 20 hours under the condition of nitrogen atmosphere. The resulted nanocapsule solution was dialyzed against DMF for purification. Various methods were utilized to examine the assembled architecture. Transferring the nanocapsules from DMF into aqueous solution was completed by dialysis. FT-IR analysis was used to confirm the success of the reaction. FT-IR spectrum for these TPyP based nanocapsules (Fig. S1b) showed that the C=N stretching band at 1594 cm^{-1} disappeared, and the bands at 1635 cm^{-1} (arrow 1) and 2932 cm^{-1} (arrow 2) corresponding to $C=N^+$ and C-H (-CH_2-) stretching appeared respectively, suggesting the monomers were covalently linked by 1, 6-dibromohexane. The zeta potential of the covalently assembled nanocapsules based on TPyP and Fe-TPyP could reach about 43.8 mV and 42.7 mV, respectively (Fig. S3 and Fig. S4), which led to the nanocapsules well soluble in aqueous solution. However, there was no obvious change on the architecture of the nanocapsules even after transferring the assemblies into water, as shown in Fig. S5a and S5b, and the assemblies presented good stability in water (Fig. S5c).
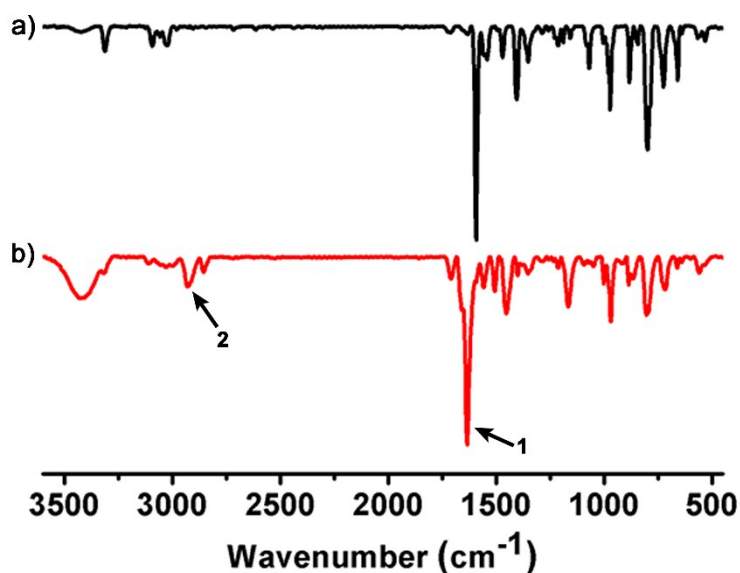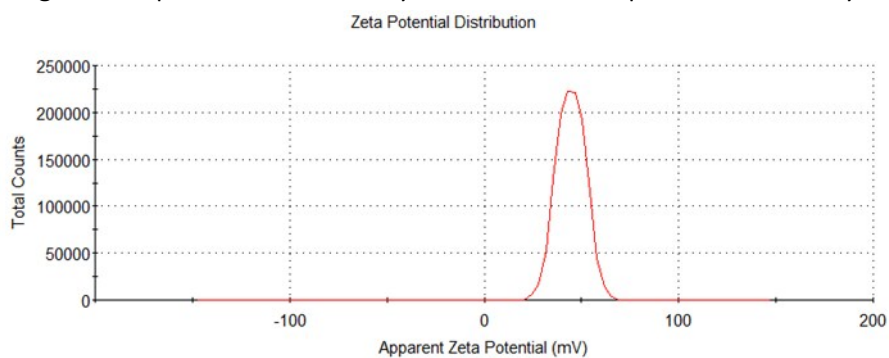

Fig. S1 FT-IR spectra of a) TPyP (black line) and b) TPyP-based nanocapsules (red line)
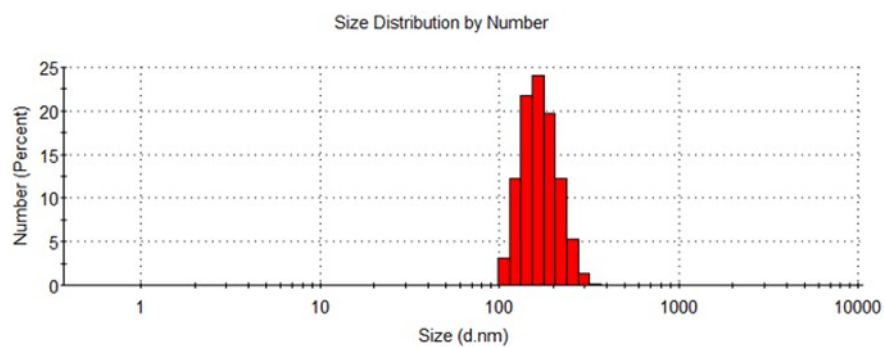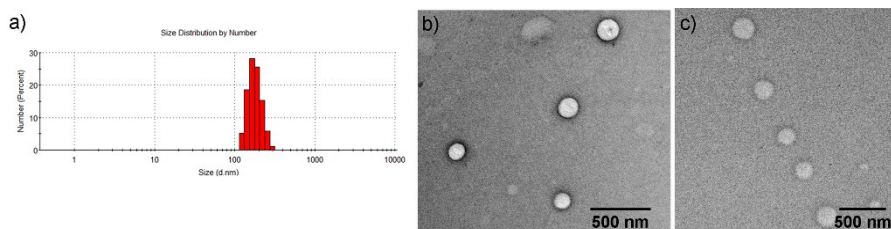
Fig. S2 DLS analysis of the TPyP based nanocapsules in DMF.
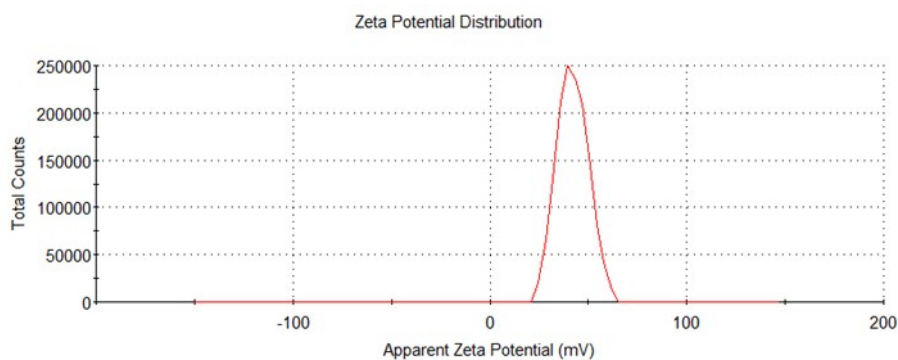
Fig. S3 Zeta potential of covalently assembled nanocapsules based on TPyP.


Fig. S4 Zeta potential of covalently assembled nanocapsules based on Fe-TPyP.

Fig. S5 Detecting the stability of the nanocapsules based on TPyP in pure water. (a) DLS and (b) TEM analysis of the freshly prepared nanocapsules in water, (c) TEM image of the nanocapsules aged for 7 days in water.

## 5. Monitoring the nanocapsule forming process using TEM

TEM was utilized to monitor the each stage of the polymerization, and the step by step formation process was observed. As shown in Fig. S5, when the reaction was carried out for 5 hours, nanosheets with the size of about 150 nm were observed, which presented some folds. After 10 hours of reaction, the formed nanosheets began to curl. When the reaction went on for 15 hours, semi-nanocapsules were detected. After 20 hours, the final morphology of hollow spheres emerged.
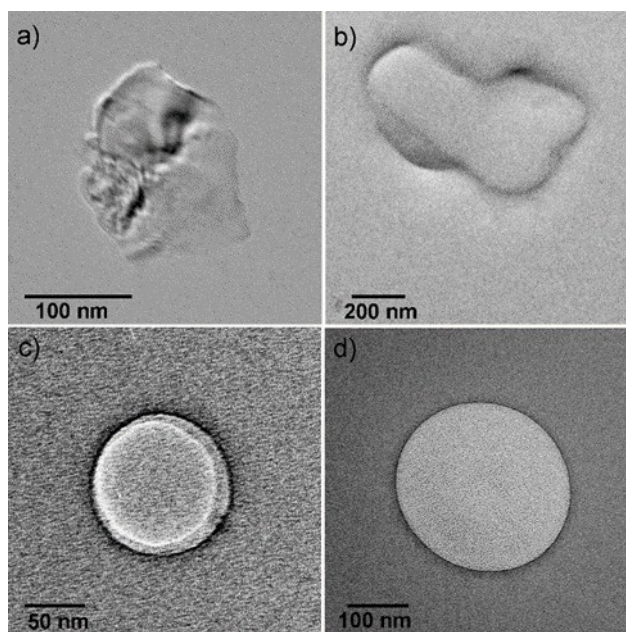
Fig. S6 HR-TEM images of the assembly when the polymerization proceeded for a) 5 hours, b) 10 hours, c) 15 hours, and d) 20 hours.

## 6. Measurement of the size of building blocks

The size of one Fe-TPyP molecule and the distance between two neighbouring Fe-THPP molecules for ordered arrangement bridged by 1, 6-dibromohexane were estimated to be 1.5 nm and 2.4 nm by a structural model in the software Gaussian, respectively.
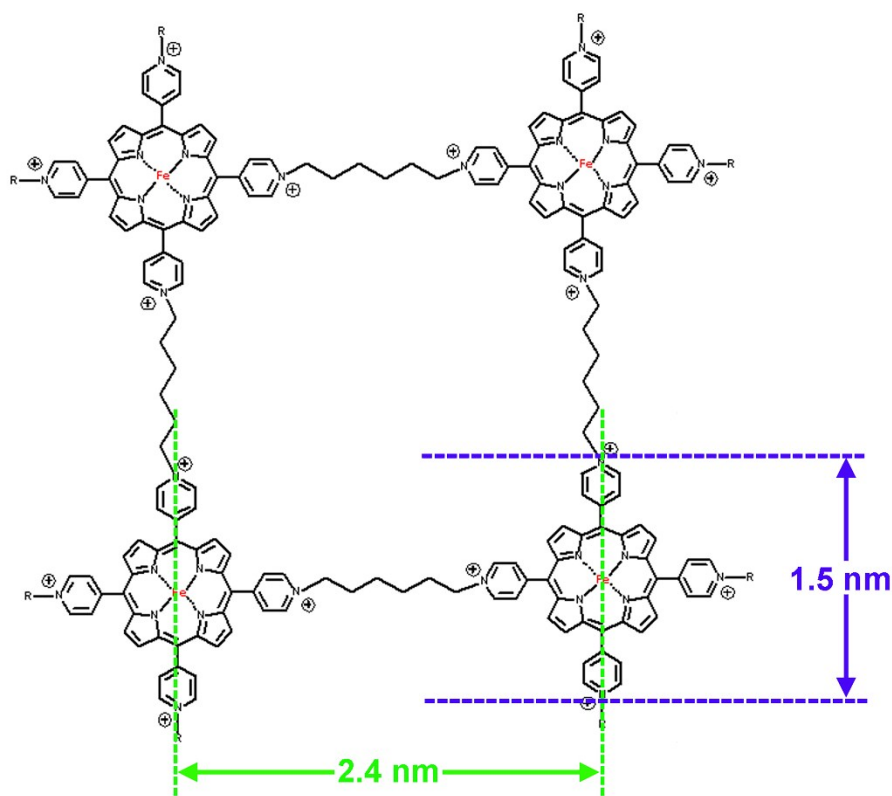
Fig. S7 The size of one Fe-TPyP molecule and the distance between two neighbouring Fe-TPyP molecules for ordered arrangement bridged by 1, 6-dibromohexane.

7. Element mapping tests

Fe element mapping was performed on the Fe-TPyP based nanosheet which presented some folds when the polymerization was carried out for 7 hours. As shown in Fig. 8b, Fe element was distributed over the whole area of the nanosheet, confirming the Fe-TPyP monomers were distributed over the whole area of the covalent assembly. The energy-dispersive X-ray spectroscopic (EDX) analysis (Fig. S8c) also revealed that the covalent assembly contained Fe element, indicating the distribution of the Fe-TPyP monomers on the assembly.
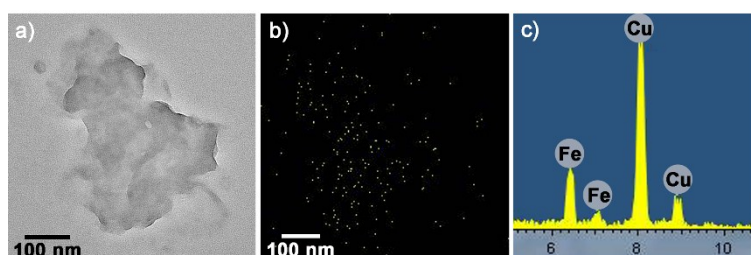

Fig. S8 a) TEM image of the nanosheet formed when the polymerization proceeded for 7 hours, b) Fe element mapping image and c) EDX analysis of the nanosheet in (a).

8. Catalytic Activity Test

To assess the catalytic capacity of the artificial enzyme, TMB oxidation catalyzed by Fe-TPyP NCs was utilized. TMB can be oxidized by H_2O_2 to produce a blue-colored product with the maximum absorption at 652 nm. We discovered that the catalytic activity of the peroxidase mimic was related to temperature and pH. The optimal pH and temperature were found to be 4.0 and 45℃～ 55℃, respectively (see Fig. S9). Furthermorer, the size of the Fe-TPyP NCs was unaltered even

when kept at pH=4 for 7 days, showing the stability of nanocapsules in detection environment (Fig. S10).
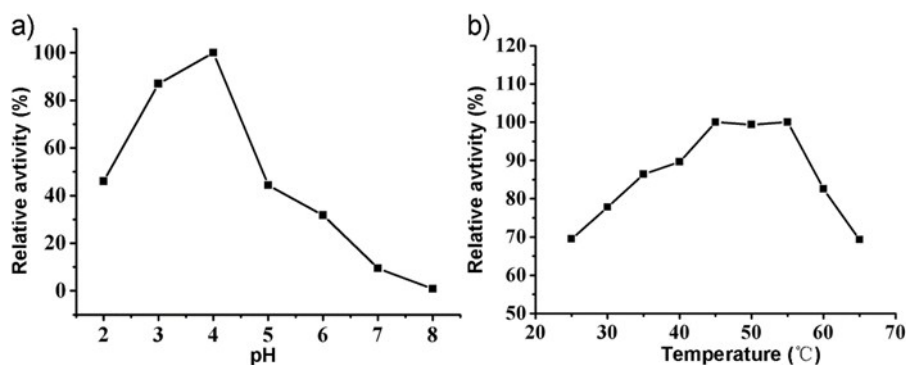
Fig. S9 Dependence of the peroxidase-like activity on (a) pH and (b) temperature. In each curve the maximum point was set as 100% (condition：2.6 μM active site equivalent, 9 mM H_2O_2, 0.8 mM TMB).
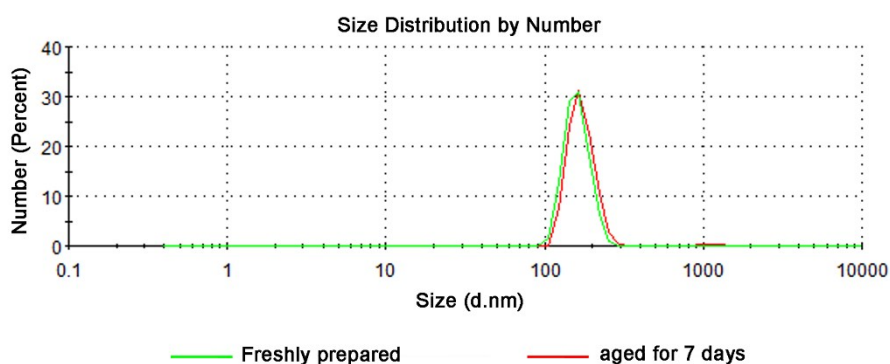
Fig. S10 Detecting the stability of the nanocapsules based on Fe-TPyP in detection environment.

The concentration of the artificial enzyme was measured by a UV-Vis spectrophotometer, and caculated using Lambert-Beer law, A=εbc (A is the absorbance of the sample, ε is the molar extinction coefficient of the sample, c is the concentration of the sample and b is the optical path length). The resulted solution of Fe-TPyP based nanocapsules was dialyzd against DMF for purification. The UV spectra of the nanocapsules were tested before and after dialyzing, and the concentration of the artificial enzyme after dialyzing was caculated using the equation of A=εbc. The oxidized product of TMB was confirmed by monitoring the absorbance at 652 nm using a UV-Vis spectrophotometer in kinetic mode. The catalytic reaction process presented typical enzymatic reaction, following the Michaelis-Menten equation:

$$V_0=V_{max} \cdot [S]/(K_M+[S])$$

where V_0 represents the initial reaction rate (the rate of forming the product), [S] represents the substrate concentration, V_{max} represents the maximum rate achieved in this system at the condition of saturating substrate concentration, K_M, the Michaelis constant, is the concentration of substrate at which the reaction rate reaches half of V_{max}. Owing to the turn over number, $k_{cat}=V_{max}/[E]$ ([E] is the enzyme concentration), the Lineweaver-Burk plot can be obtained as follows:

$$1/V_0=K_M/(k_{cat} \cdot [E] \cdot [S])+1/(k_{cat} \cdot [E])$$

from which significant kinetic parameters, k_{cat} and K_M can be obtained.

Through varying the concentration of one substrate and maintaining the concentration of the other fixed, we found that the catalytic reaction process for Fe-TPyP NCs as the catalysts presented typical enzymatic reaction, following the Michaelis-Menten equation (Fig. S11a for TMB and Fig. S11c for H_2O_2). According to the Lineweaver-Burk plot, which presented a nearly excellent linear relationship through linear fitting (Fig. S11b for TMB and Fig. S11d for H_2O_2), significant apparent kinetic parameters, K_M and k_{cat} can be obtained. In addition, we assessed the catalytic activity of the water-soluble monomers, Fe-TMPyP (see Fig. S12), the test method was the same as that in the catalytic test for Fe-TPyP NCs as the catalysts.
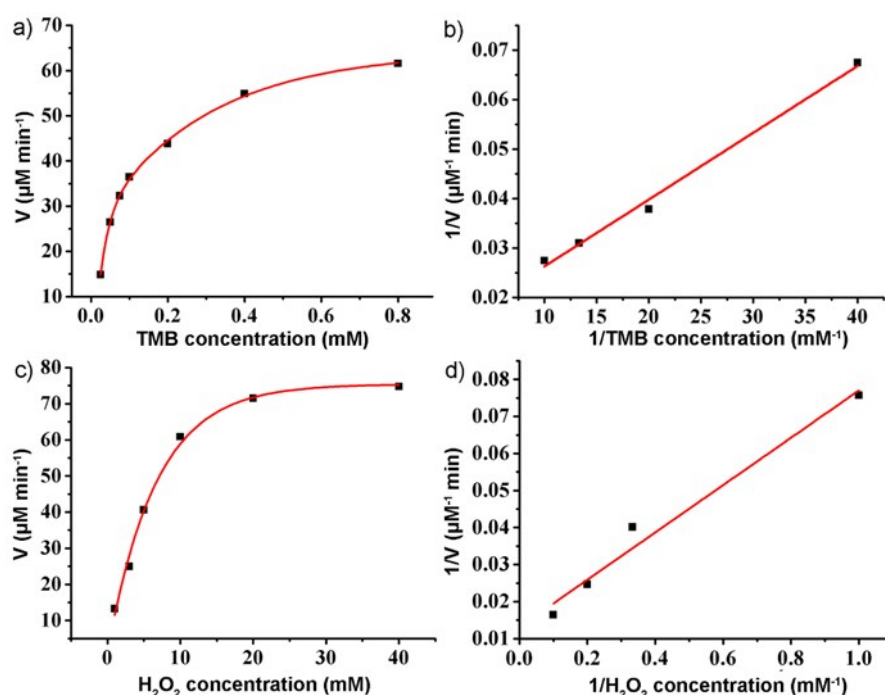
Fig. S11 Steady-state kinetic assays of Fe-TPyP NCs. (a) Michaelis–Menten and (b) Lineweaver-Burk plots for the TMB substrate (2.6 µM active site equivalent, 9 mM H_2O_2, pH=4.0, TMB concentration was varied). (c) Michaelis–Menten and (d) Lineweaver–Burk plots for the H_2O_2 substrate (2.6 µM active site equivalent, 0.8 mM TMB, pH=4.0, H_2O_2 concentration was varied).
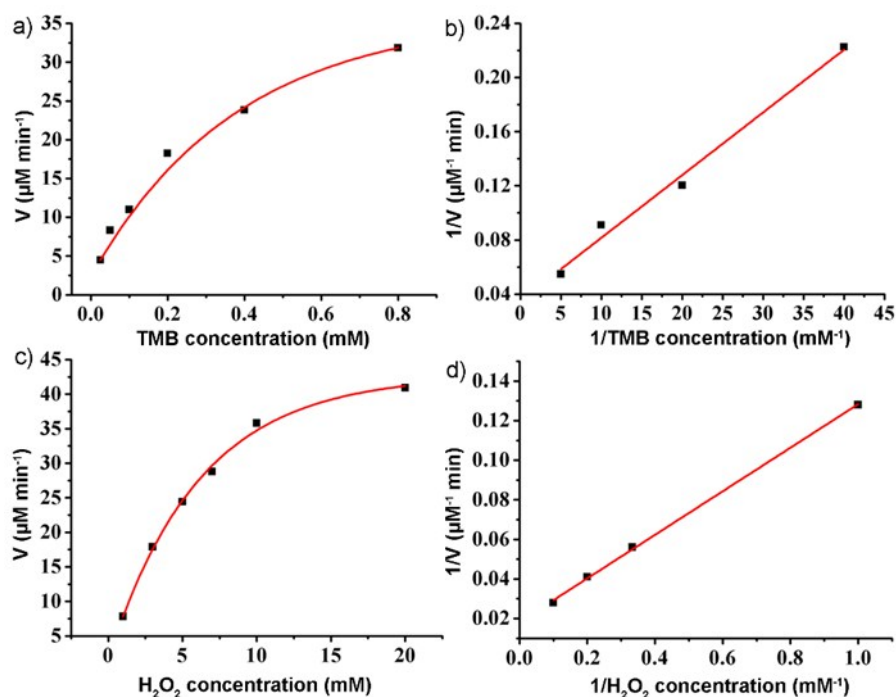
Fig. S12 Steady-state kinetic assays of Fe-TMPyP. (a) Michaelis–Menten and (b) Lineweaver-Burk plots for the TMB substrate (2.5 μM active site equivalent, 9 mM H_2O_2, pH=4.0, TMB concentration was varied). (c) Michaelis–Menten and (d) Lineweaver–Burk plots for the H_2O_2 substrate (2.5 μM active site equivalent, 0.8 mM TMB, pH=4.0, H_2O_2 concentration was varied).

The fabricated peroxidase mimic can be collected through ultrafiltration centrifugation, and it can be reused without losing its enzymatic activity (Table S1).

Table S1 Recyclability of Fe-TPyP based nanocapsules for the oxidation of TMB.

Number of catalytic cycles	1	2	3
Activity[a] (μM min⁻¹ μM⁻¹)	3.92	3.85	3.78

[a] The enzymatic reaction was conducted at pH=4.0 in the presence of 2.6 μM iron-porphyrin monomers, 2 mM H_2O_2 and 0.2 mM TMB.

9. The detection of glucose

100 μL of 1mg/mL GOX aqueous solution and 100 μL of different concentration of glucose PBS buffer solution (pH=6.7, 10 mM) were mixed together and incubated at 37 ℃ for 50 min. Then, 240 μL of PBS buffer solution (pH=4.0, 100 mM)，10 μL of Fe-TPyP based nanocaspules aqueous solution (130 μmol active site equivalent) and 50 μL of TMB ethanol solution (8 mM) were added into the above mixture and incubated at 37 ℃ for another 50 min. The mixture was then applied for spectral measurement.

10. Comparing this work with selected nanomaterial based colorimetric determination for glucose

Table S2 Comparison of the determination for glucose based on different nanomaterials.

Catalyst	Linear range (µM)	LOD (µM)	Reference
Hemin functionalized graphene nanosheets	0.05-500	0.03	2
Graphene Oxide	1-20	1	3
Casein-Fe3O4	3-1000	1	4
Pt Nanoclusters	0-200	0.28	5
Carbon nanodots	1-500	0.4	6
BSA-Cu NCs	100-2000	100	7
ZnFe2O4	1.25-18.75	0.3	8
Fe-TPyP nanocapsules	0.24-15.6	0.098	This work

References

1. M. Natali, A. Luisa, E. Iengo and F. Scandola, *Chem. Commun.*, 2014, **50**, 1842.
2. Y. Guo, J. Li and S. Dong, *Sensors and Actuators B*, 2011, **160**, 295.
3. Y. Song, K. Qu, C. Zhao, J. Ren and X. Qu, *Adv. Mater.*, 2010, **22**, 2206.
4. Y. Liu, M. Yuan, L. Qiao and R. Guo, *Biosens. Bioelectron.*, 2014, **52**, 391.
5. L. Jin,,Z. Meng, Y. Zhang, S. Cai, Z. Zhang, C. Li, L. Shang and Y. Shen, *ACS Appl. Mater. Interfaces*, 2017, **9**, 10027.
6. W. Shi, Q.Wang, Y. Long, Z. Cheng, S. Chen, H. Zheng and Y. Huang, *Chem. Commun.*, 2011, **47**, 6695.
7. L. Hu, Y. Yuan, L. Zhang, J. Zhao, S. Majeed and G. Xu, *Anal. Chim. Acta*, 2013, **762**, 83.
8. L. Su, J. Feng, X. Zhou, C. Ren, H. Li and X. Chen, *Anal. Chem.*, 2012, **84**, 5753.